# Direct observation of individual endogenous protein complexes *in situ* by proximity ligation

Ola Söderberg[1,3], Mats Gullberg[1,3], Malin Jarvius[1,3], Karin Ridderstråle[2], Karl-Johan Leuchowius[1], Jonas Jarvius[1], Kenneth Wester[1], Per Hydbring[2], Fuad Bahram[2], Lars-Gunnar Larsson[2] & Ulf Landegren[1]



**Cellular processes can only be understood as the dynamic interplay of molecules. There is a need for techniques to monitor interactions of endogenous proteins directly in individual cells and tissues to reveal the cellular and molecular architecture and its responses to perturbations. Here we report our adaptation of the recently developed proximity ligation method to examine the subcellular localization of protein-protein interactions at single-molecule resolution. Proximity probes—oligonucleotides attached to antibodies against the two target proteins—guided the formation of circular DNA strands when bound in close proximity. The DNA circles in turn served as templates for localized rolling-circle amplification (RCA), allowing individual interacting pairs of protein molecules to be visualized and counted in human cell lines and clinical specimens. We used this method to show specific regulation of protein-protein interactions between endogenous Myc and Max oncogenic transcription factors in response to interferon-γ (IFN-γ) signaling and low-molecular-weight inhibitors.**

To achieve the specificity and sensitivity required to directly observe interacting endogenous proteins in cells and subcellular compartments, single proteins must yield easily detectable signals, whereas nonspecific background noise must be reduced to negligible levels. For this purpose, we adapted the proximity ligation technique[1,2] for highly specific *in situ* detection coupled to a localized amplification reaction. The proximity ligation method depends on the dual proximal binding by pairs of detection reagents to generate amplifiable DNA strands, which then serve as surrogate markers for the detected protein molecules[1,2]. We combined proximity ligation with RCA for localized readout in fixed cells or tissues. The oligonucleotides on the proximity probes, when brought into close proximity by binding adjacent proteins, serve as templates for the circularization of so-called connector oligonucleotides by enzymatic ligation. The circularized DNA strands remain hybridized to the proximity probes. Upon addition of phi29 DNA polymerase, one of the oligonucleotides serves as a primer for the RCA reaction, in the process unwinding the other oligonucleotide from the DNA circle. The oligonucleotide of the other proximity probe has three mismatched, exonuclease-resistant 2′*O*-methyl RNA nucleotides at the 3′ end, preventing it from serving as a primer for RCA. A 1-h RCA reaction generates a randomly coiled, single-stranded product composed of up to 1,000 complements of the DNA circle[3], covalently linked to an antibody-antigen complex. This product is easily detected through hybridization of complementary fluorescence-labeled oligonucleotides (**Fig. 1a**).

We used this proximity ligation *in situ* assay (P-LISA) to investigate the well-characterized interaction between the transcription factor and oncoprotein c-Myc and its obligatory partner protein Max. c-Myc and Max heterodimerize through their basic helix-loop-helix leucine-zipper domains, thereby enabling the c-Myc/Max complex to bind DNA recognition elements at targeted gene promoters. c-Myc–dependent recruitment of coactivator complexes leads to activation of numerous genes involved in fundamental cellular processes, such as proliferation, apoptosis, metabolism, differentiation and genomic stability[4–6]. Deregulation of Myc-family genes resulting in uncontrolled cell growth is frequently observed in tumors[7]. Although the Myc network has been extensively studied, there has been a lack of techniques to monitor the interactions and the subcellular localization of endogenous c-Myc and Max proteins or any other protein complexes. Coimmunoprecipitation and other protein pull-down assays allow stable protein interactions to be investigated in cell populations, but they do not easily reveal transient interactions and the distribution of interacting proteins between or within individual cells. In contrast, techniques such as bimolecular fluorescence complementation[8] reflect the subcellular localization of protein interactions but require the proteins to be ectopically expressed as fusion proteins at high levels. Here we show that the P-LISA method enables the localized detection of individual, endogenous, interacting protein pairs in fixed cultured cells, cytospin preparation, and tissue sections, thus providing an important new tool for use in basic and clinical research.

## RESULTS

### Visualizing endogenous protein-protein interactions

We applied the P-LISA technique to investigate interactions between endogenous c-Myc/Max proteins in various cell types

[1]Department of Genetics and Pathology, Rudbeck Laboratory, University of Uppsala, SE-75185 Uppsala, Sweden. [2]Department of Plant Biology and Forest Genetics, Uppsala Genetic Center, Swedish University of Agricultural Sciences, SE-75007, Uppsala, Sweden. [3]These authors contributed equally to this work. Correspondence should be addressed to U.L. (ulf.landegren@genpat.uu.se).

RECEIVED 9 MAY; ACCEPTED 5 SEPTEMBER; PUBLISHED ONLINE 29 OCTOBER 2006; DOI:10.1038/NMETH947

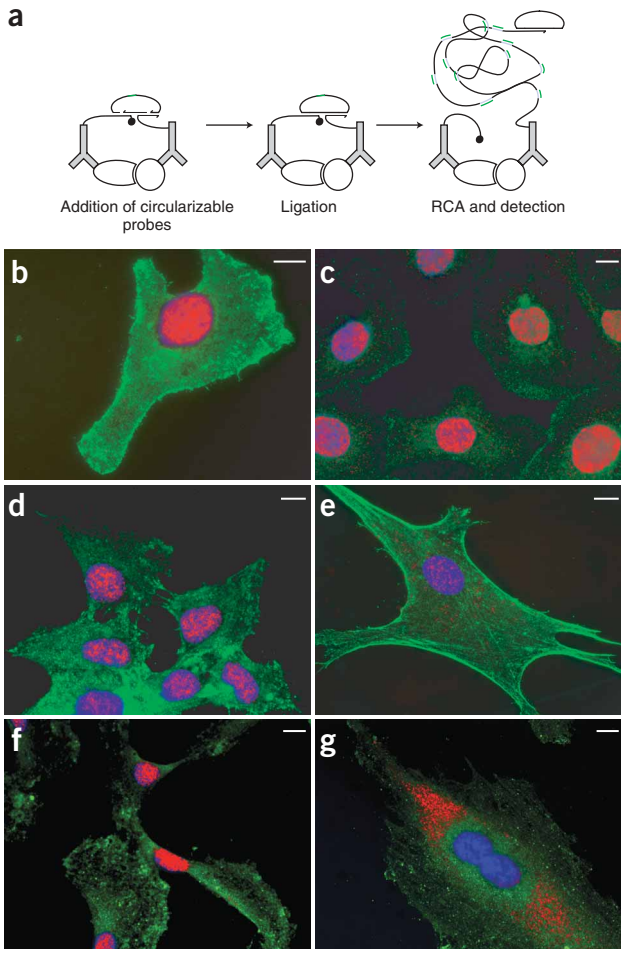


**Figure 1** | Detection of endogenous c-Myc/Max heterodimers in cultured cells using P-LISA. (**a**) Schematic presentation of proximity probe–templated DNA circularization and subsequent RCA and detection. If two proximity probes bind close to each other, such as by binding two proteins present in the same complex, then subsequently added linear connector oligonucleotides are guided to form a circular structure covalently joined by enzymatic DNA ligation. After ligation, RCA is initiated using one of the proximity probes as a primer. The RCA product is detected through hybridization of fluorescence-labeled oligonucleotides complementary to a tag sequence in the RCA product. The filled circle represents the blocked 2′-*O*-methyl RNA 3′ end of the nonpriming proximity probe. The green line in the circle that forms the proximity ligation reaction gives rise to multiple copies of complementary sequence in the RCA product (blue). This motif is detected by hybridizing fluorescence-labeled detection oligonucleotides (green). (**b–g**) c-Myc/Max heterodimers were visualized by staining cells with proximity probes directed against c-Myc and Max, followed by ligation and RCA as outlined in **a**. The hybridization probes were labeled with Alexa 555 (red), the cytoplasm was counterstained with FITC-labeled antibody to actin (green) and the nuclei were stained with Hoechst 33342 (blue). Scale bar represents 10 μm. The c-Myc/Max heterodimers were detected in U2OS cells (**b**), Skov-3 cells (**c**), CHO-K1 cells (**d**), normal human fibroblasts (**e**), TIME cells (**f**) and TIME cells during mitosis (**g**).

and observed strong fluorescence signals in U2OS human osteosarcoma cells (**Fig. 1b**), Skov-3 human ovary adenocarcinoma cells (**Fig. 1c**), CHO-K1 Chinese hamster ovary cells (**Fig. 1d**), normal human fibroblasts (**Fig. 1e**) and telomerase-immortalized human microvascular endothelial (TIME) cells[9] (**Fig. 1f**,**g**). As expected from the nuclear localization of c-Myc and of c-Myc/Max heterodimers previously identified by bimolecular fluorescence complementation[10], the P-LISA signals were predominantly present in the cell nuclei, except in mitotic cells (**Fig. 1g**), which showed a strict cytopolar staining pattern[11]. The presence of prominent signals in Rat1 TGR-1 fibroblasts (**Fig. 2a**) and absence of signals in the corresponding c-*myc* knockout cells[12] (**Fig. 2b**) confirmed the strict dependence on dual recognition of c-Myc/Max heterodimers to yield signals. Additionally, we observed no RCA products in U2OS cells when a proximity probe directed against the epidermal growth factor receptor (EGFR), which does not interact with c-Myc, was substituted for the anti-Max reagent (**Fig. 2c**). In contrast, the EGFR probe did yield RCA products when combined with a probe against Her-2, revealing the known colocalization of these two cell-surface proteins[13] (**Fig. 2d**).

To investigate whether the assay is sufficiently sensitive to permit detection of individual c-Myc/Max heterodimers, we simultaneously applied two variants of one of the connector oligonucleotides. Under this condition, distinct fluorescent probes would hybridize to the RCA products depending on whether one or the other connector fragment was included in the DNA circles that formed. The spots consistently exhibited one of the two fluorescent colors but not both, confirming that they were composed of single RCA products and that the signals originated from individual c-Myc/Max molecule pairs (**Fig. 2e**).

The induction of transcription of Myc-regulated genes depends on chromatin remodeling at the promoters by the c-Myc complex, while RNA polymerase II may be recruited through the Akt pathway[14,15]. c-Myc has been reported to interact with mediator subunits of the RNA polymerase II holoenzyme and with other components of the preinitiation complex[15], suggesting that the c-Myc/Max and RNA polymerase II complexes may be in close proximity at the promoter, although c-Myc/Max binding sites are often found several kilobases away from the transcriptional binding site. We therefore modified the P-LISA design to detect three interacting proteins. We detected c-Myc/Max heterodimers located near the RNA polymerase, with proximity probes directed at each of the three proteins binding in proximity and giving rise to an amplifiable detection reaction (**Fig. 2f**). This allowed us to observe endogenous interactions between the DNA-binding activator complex c-Myc/Max with RNA polymerase II in the SHSY5Y neuroblastoma cell line *in situ*, possibly reflecting induction of transcription of endogenous Myc-regulated genes (**Fig. 2g**).

We next used the P-LISA technique to investigate tissue sections from clinical material. Staining for c-Myc/Max interactions in frozen tissue sections from normal colon revealed abundant signals in a subpopulation of colon crypt epithelial cells (**Fig. 3a**). The pattern of c-Myc/Max interactions was associated with c-Myc expression in the same tissue, as determined by conventional enzyme-based immunostaining (**Fig. 3b**). Interactions between c-Myc and Max in human tonsil tissue were restricted to a subpopulation of cells (**Fig. 3c**), in contrast to tissue sections from a sample of Burkitt lymphoma. This B-cell lymphoma is characterized by translocation of the gene encoding c-Myc to one of the immunoglobulin loci, resulting in deregulated c-Myc expression. The vast majority of cells in the Burkitt lymphoma sample stained positively for the presence of c-Myc/Max heterodimers (**Fig. 3d**).

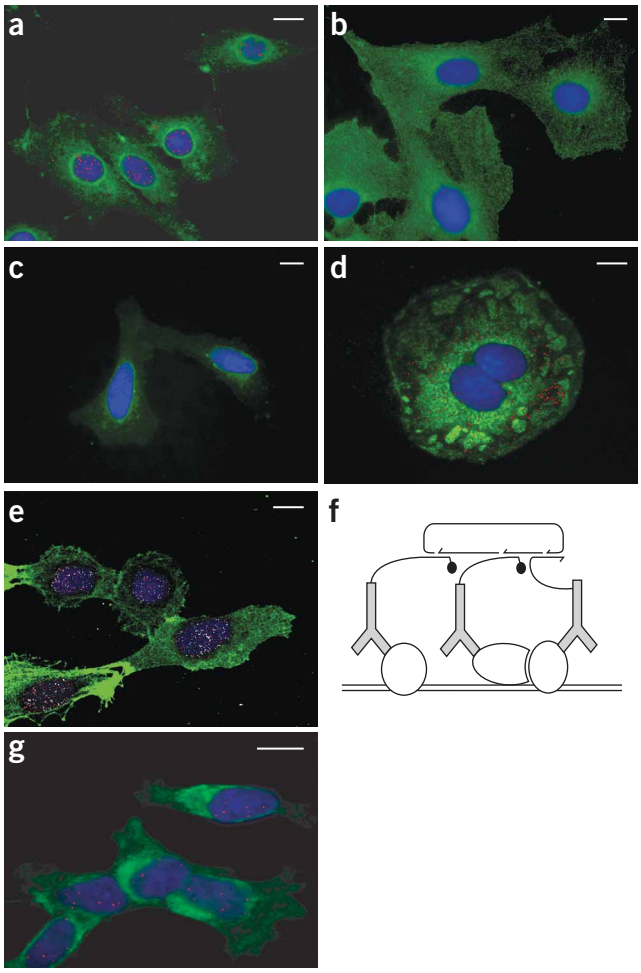


**Figure 2** | Detection of protein-protein interactions. c-Myc/Max heterodimers were visualized using hybridization probes labeled with Alexa 555 (red). The cytoplasm was stained with FITC-labeled antibody to actin (green), and the nuclei were stained with Hoechst 33342 (blue). Scale bar represents 10 μm. (**a**) Staining of Rat1 TGR-1 cells. (**b**) Staining of Rat 1 c-Myc knockout cells (HO15.19, *myc*$^{-/-}$). (**c**) Staining of U2OS cells with one of the two proximity probes directed against an irrelevant target (EGFR) together with a c-Myc probe. (**d**) Detection of EGFR together with a Her-2 probe. (**e**) Staining of U2OS cells in which individual RCA products were detected by hybridization with either of two hybridization probes labeled with Alexa 555 and Cy5. Individual spots characterized by one or the other color are likely to be the products of amplification of single DNA circles. (**f**) Schematic presentation of proximity probe–templated DNA circularization using three proximity probes. (**g**) c-Myc/Max/RNA polymerase II interactions were visualized in SHSY5Y cells by P-LISA using hybridization probes labeled with Alexa 555 (red). The cytoplasm was stained with FITC-labeled antibody to actin (green), and the nuclei were stained with Hoechst 33342 (blue). Scale bar represents 10 μm.



## Monitoring perturbations of Myc/Max interactions

Previous studies have shown that transformation of human U-937 monoblasts with a potent viral form of Myc (v-Myc) abrogates differentiation and cell cycle arrest induced by 12-*O*-tetradecanoyl-phorbol-13-acetate TPA, vitamin D3 or retinoic acid. IFN-γ restores the response to these agents, resulting in terminal differentiation and cell cycle arrest in transformed U-937 cells and in cell lines derived from patients with N-*myc*–amplified neuroblastomas. This occurs in both cases despite constitutive *myc* mRNA and Myc protein expression[16,17]. Subsequent studies showed that IFN-γ inhibits Myc activity by destabilizing Myc/Max heterodimers[18]. We used the P-LISA method to monitor Myc/Max interactions in individual U-937 monoblasts and observed a profound decrease in Myc/Max heterodimers after treatment with IFN-γ in combination with TPA (**Fig. 4a–c**). Notably, the Myc/Max interactions that remained after treatment with IFN-γ and phorbol esters were predominantly localized in the cytoplasm of treated cells, suggesting that Myc/Max heterodimers were either formed in the cytoplasm or exported out of the nucleus before Myc/Max dissociation or that the IFN-γ–induced dissociation signals acted solely in the nucleus. The visualization of individual proteins or protein complexes as distinct fluorescent spots by P-LISA allowed quantitative effects to be digitally recorded by computer-assisted image analysis, increasing both throughput and objectivity of measurement (**Fig. 4c**).

To verify that P-LISA specifically measures c-Myc/Max heterodimers, we used the well-known Myc-estrogen receptor (MycER) system, where c-Myc is fused to the ligand-binding domain of ER[19–21]. In the absence of ligand, Max is precluded from interacting with c-Myc by Hsp90, which is displaced after stimulation of the cells with 4-OH-tamoxifen[21]. The expression of MycER was similar in stimulated cells and controls, as determined by P-LISA using a pair of proximity probes directed against c-Myc and ER (**Fig. 4d**). However, using the c-Myc and Max proximity probes, we observed a considerable increase in signal in 4-OH-tamoxifen–stimulated cells over the endogenous levels detected in unstimulated cells, confirming that P-LISA specifically reported the presence of c-Myc/Max heterodimers.

Recently, a series of small molecules have been described that specifically inhibit c-Myc/Max association in a yeast two-hybrid system, interfere with transcription, cell growth in culture and *in vivo* tumor formation induced by c-Myc in cells[22], and efficiently

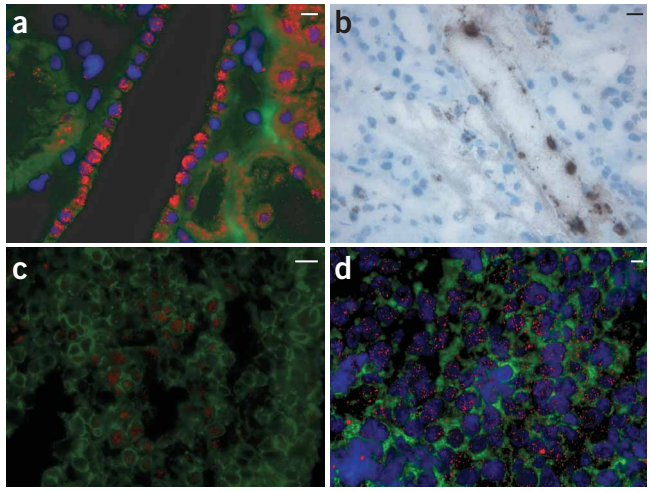


**Figure 3** | Visualization of c-Myc/Max heterodimerization in tissue sections. In all panels except **b**, c-Myc/Max heterodimers were visualized in zinc-fixed frozen tissue sections by staining cells with proximity probes directed against c-Myc and Max, followed by ligation and RCA. The hybridization probes were labeled with Alexa 555 (red), the cytoplasm was counterstained with FITC-labeled antibody to actin (**a**; green) or CD45 (**c**,**d**; green) and the nuclei were stained with Hoechst 33342 (blue). Scale bar represents 10 μm. (**a**) Staining of a tissue section of normal human colon. (**b**) Regular immunostaining for c-Myc expression in normal human colon. (**c**) Staining of a tissue section from human tonsil. (**d**) Staining of a tissue section from a sample of Burkitt lymphoma.

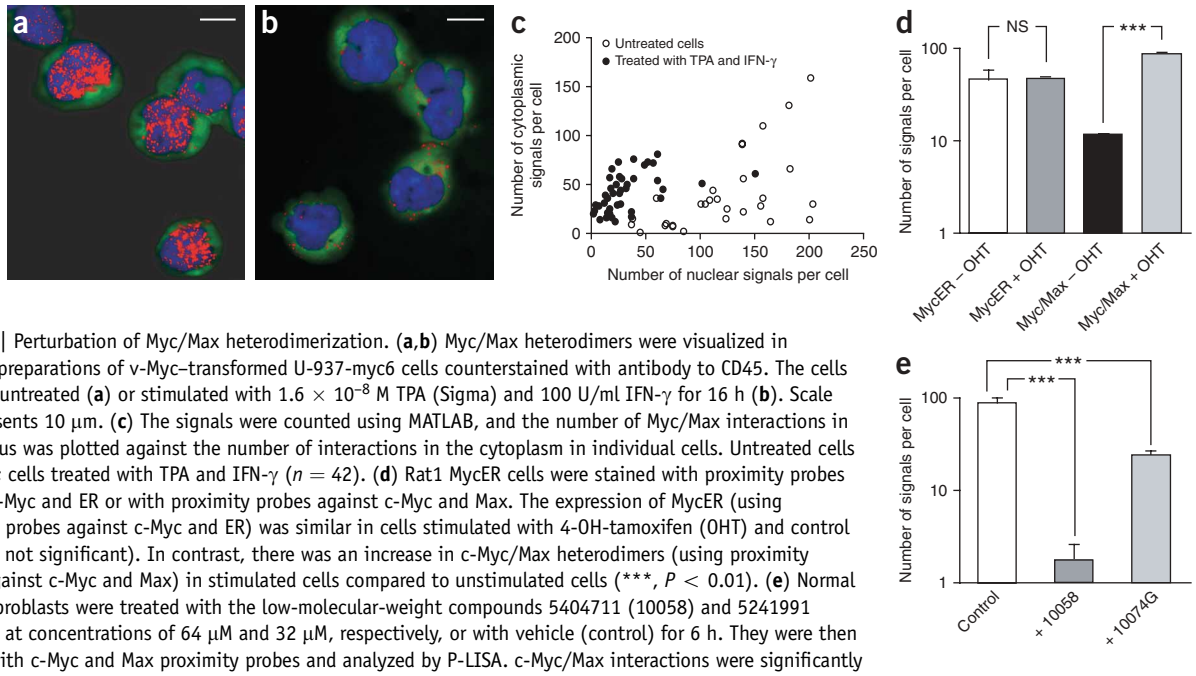


**Figure 4** | Perturbation of Myc/Max heterodimerization. (**a**,**b**) Myc/Max heterodimers were visualized in cytospin preparations of v-Myc–transformed U-937-myc6 cells counterstained with antibody to CD45. The cells were left untreated (**a**) or stimulated with $1.6 \times 10^{-8}$ M TPA (Sigma) and 100 U/ml IFN-γ for 16 h (**b**). Scale bar represents 10 μm. (**c**) The signals were counted using MATLAB, and the number of Myc/Max interactions in the nucleus was plotted against the number of interactions in the cytoplasm in individual cells. Untreated cells ($n = 29$); cells treated with TPA and IFN-γ ($n = 42$). (**d**) Rat1 MycER cells were stained with proximity probes against c-Myc and ER or with proximity probes against c-Myc and Max. The expression of MycER (using proximity probes against c-Myc and ER) was similar in cells stimulated with 4-OH-tamoxifen (OHT) and control cells (NS, not significant). In contrast, there was an increase in c-Myc/Max heterodimers (using proximity probes against c-Myc and Max) in stimulated cells compared to unstimulated cells (***, $P < 0.01$). (**e**) Normal human fibroblasts were treated with the low-molecular-weight compounds 5404711 (10058) and 5241991 (10074G) at concentrations of 64 μM and 32 μM, respectively, or with vehicle (control) for 6 h. They were then stained with c-Myc and Max proximity probes and analyzed by P-LISA. c-Myc/Max interactions were significantly inhibited by 10058 and 10047G (***, $P < 0.01$ for both) compared to control. Statistical analyses were performed using ANOVA with Dunnett's correction ($P < 0.0001$).



repress c-Myc–induced transcription of DNA encoding ribosomal RNA by RNA polymerase I (ref. 23). The effects of the inhibitors on authentic c-Myc/Max interactions, however, have not been shown in any cell system. Using P-LISA, we showed that the experimental compound 10058 very efficiently inhibited endogenous c-Myc/Max interactions in normal cultured human fibroblasts to 2% of the control level (**Fig. 4e**). The compound 10074G inhibited the interaction less efficiently but to a still-significant 27% of the control level (**Fig. 4e**). We confirmed these results by coimmunoprecipitation (data not shown). These observations extend published findings[22,23] by showing the efficacy of the compounds in inhibiting the formation of endogenous c-Myc/Max heterodimers in cells. The P-LISA technique therefore has potential for monitoring the response to molecular therapies targeting protein-protein interactions in any cells or tissues.

## DISCUSSION

The ability to detect the intra- and intercellular distribution of endogenous proteins at the single-molecule level using P-LISA will be valuable for studies of biological processes such as regulation of proliferation, differentiation and survival in complex microenvironments. Moreover, because it is possible to increase the number of proximity probes used to create a circular amplifiable ligation product, P-LISA is uniquely suited to study multiprotein complexes such as the ternary c-Myc/Max/RNA polymerase II complexes demonstrated here. Because samples are fixed before analysis, snapshots of cellular processes are obtained, and transient interactions can therefore be easily detected. P-LISA offers at least two advantages over such methods as fluorescence or bioluminescence resonance energy transfer and bimolecular fluorescence complementation. First, endogenous proteins can be investigated; and second, signal amplification by RCA increases the number of fluorophores per detected protein interaction, so that single events can be easily visualized as prominent fluorescent spots while ignoring any nonspecifically bound fluorescent probes. At present, we have no measure of the efficiency of detection by P-LISA, but we expect that only a fraction of the molecules present in a cell are detected as fluorescent spots.

By varying the protein binders (such as intact antibodies or $F_{ab}$ fragments) and the lengths of the oligonucleotides on the proximity probes, P-LISA could theoretically be used as a molecular ruler, allowing measurements of distances between epitopes. The maximum distance between determinants recognized by P-LISA here was estimated at roughly 30 nm, including the size of the two antibodies and the oligonucleotides connecting them in the detected protein pairs. If required, substantially longer distances could be spanned using longer oligonucleotides, or more compact binders and shorter DNA sequences could be used to improve resolution by limiting detection distances to just over 10 nm. This is comparable to the distance at which resonance energy transfer occurs between fluorophores (5–10 nm). The method could also be modified to detect interactions between proteins and other molecules, such as specific DNA or RNA sequences (O.S. *et al.*, unpublished observations).

In conclusion, P-LISA confers dual-binder specificity for protein detection *in situ* and can reveal interactions between proteins directly in normal cells and tissues without being subject to artifacts of overexpression or ectopic expression. This method should contribute to the establishment and use of comprehensive interactome maps in basic research and for clinical diagnosis.

## METHODS

**Preparation of proximity probes.** The proximity probes consisted of affinity-purified polyclonal or monoclonal antibodies modified by covalently attachment of the 5′ end of various oligonucleotides to each antibody. For each conjugation, we dialyzed 20 μg of antibody, c-Myc (sc-764X, sc-40X), Max (sc-197X, sc-765X),

RNA polymerase II (sc-9001X) and either ER (sc-787) or EGFR and Her-2 (Merck) overnight against PBS using Slide-A-Lyzer MINI dialysis unit (Pierce Biotechnology). This was followed by a 2-h incubation with a 30-fold excess of sulfosuccinimidyl-4-(*N*-maleimidomethyl) cyclohexane-1-carboxylate (sulfo-SMCC; Pierce), freshly prepared in DMSO, in 55 mM phosphate buffer, 150 mM NaCl and 20 mM EDTA (pH 7.2). In parallel, we reduced 300 pmol of the thiol-modified, nonpriming proximity probe oligonucleotide SH-AAAAAAAAAAGACGCTAATAGTTAAGACGCTT [UUU] (the sequence within the brackets is 2′*O*-methyl-RNA) or, for the experiment in **Figure 2g**, the oligonucleotide SH-AAAAAA AAAAATGGCCGACTCACGAATTAGA [UUU] or the RCA primer proximity probe oligonucleotide SH-AAAAAAAAAATATGA CAGAACTAGACACTCTT (purchased from Eurogentec) with 10 mM DTT (Sigma) in 55 mM phosphate buffer, 150 mM NaCl and 20 mM EDTA (pH 7.2) for 1 h at 37 °C. We purified the reactions using MicroSpin G-50 columns (Amersham Biosciences) that had been equilibrated with 5 mM EDTA in PBS at 735 *g* for 1 min. We then mixed the purified antibodies and oligonucleotides and incubated them overnight at 4 °C for conjugation (see **Supplementary Protocol** online).

**Cell cultures and tissue sections.** We cultured GM08402 normal human fibroblasts (purchased from Coriell Cell Repositories) in MEM with 10% FBS, U2OS cells in McCoy 5A with 10% FBS, CHO-K1 and Skov-3 cells in RPMI 1640 with 10% FBS, SHSY5Y in DMEM with 20% FBS, and TIME cells[9] in MV2 endothelial-cell basal medium (PromoCell) supplemented with penicillin and streptomycin on Lab-Tek chamber slides (Nalge Nunc International). Six hours before the collection of GM08402 cells that had been cultured on growth factor–reduced, Matrigel-coated Lab-Tek chamber slides (BD Biosciences), we added the low-molecular-weight inhibitors 5404711 (10058) and 5241991 (10074G; ChemBridge), at concentrations of 64 μM and 32 μM, respectively. We washed the slides in TBS and fixed them with zinc fix[24] overnight for all experiments, except the one shown in **Figure 2d** in which we fixed slides with 1% paraformaldehyde (Sigma), and washed them with TBS before staining. We cultured Rat1 TGR (*myc*$^{+/+}$) and HO15.19 (*myc*$^{-/-}$) cells[12] and Rat1 MycER cells[19] in DMEM with 10% FBS supplemented with penicillin and streptomycin. We serum-starved the Rat1 Myc-ER cells on chamber slides in DMEM with 0.3% FBS for 48 h before a 6-h stimulation with 200 nM 4-OH-tamoxifen (Sigma). We rinsed the slides with TBS and fixed them with zinc fix overnight. We cultured U937-myc6 cells, infected with a v-*myc*–containing retrovirus[16], and thus constitutively expressing the v-Myc protein, in RPMI 1640 with 10% FBS supplemented with penicillin and streptomycin and stimulated with $1.6 \times 10^{-8}$ M TPA (Sigma) and 100 U/ml IFN-γ for 16 h. After washing the cells in TBS, we made cytospin preparations that were air-dried for 30 min and fixed with zinc fix overnight[24].

We placed tissue sections from frozen colon tissues on Superfrost Plus slides (Erie Scientific Company) and zinc-fixed them overnight. To prevent the tissue sections from falling off during staining, we placed the zinc-fixed frozen tissue sections of human tonsil and Burkitt lymphoma on plain glass slides and covered them with a thin film of 0.5% agarose.

**P-LISA reactions.** We blocked the slides with zinc-fixed cells or tissues by treatment with 4% normal rabbit serum (Jackson ImmunoResearch), 250 ng/μl BSA (New England Biolabs), 50 ng/μl RNase A (Promega), 11 ng/μl poly(A) (Sigma) and 0.05% Tween-20 in TBS for 2 h at 37 °C before overnight incubation at 4 °C with 2.5 ng/μl proximity probes, 7.5 ng/μl poly(A), 2.5 mM cysteine (Sigma), 250 ng/μl BSA and 0.05% Tween-20 in TBS with 5 mM EDTA. We then added two connector oligonucleotide probes (P-CTATTAGCGTCCAGTGAATGC GAGTCCGTCTAAGAGAGTAGTACAGCAGCCGTCAAGAGTGT CTA and P-GTTCTGTCATA TTTAAGCGTCTTAA) at 125 nM in 10 mM Tris-acetate (pH 7.5), 10 mM magnesium acetate, 50 mM potassium acetate, 0.05 U/μl T4 DNA ligase (Fermentas), 250 mM NaCl, 250 ng/μl BSA and 0.05% Tween-20 in $H_2O$ and ligated the probes to form circles using as templates the two oligonucleotides attached to the antibodies. In the experiment shown in **Figure 2e**, we also used the connector oligonucleotide probe P-CTATTAGCG TCAGCGATCTGCGAGACCGTATAAGAGAGTAGTACAGCAGCC GTCAAGAGTGTCTA. In the experiment shown in **Figure 2g**, we replaced the short connector oligonucleotide with two oligonucleotides (P-GTTCTGTCATATTTATCTAATTCGT and P-GAGTCGGC CATAGTATCCTTTAAGCGTCTTAA), both at 125 nM. We performed ligations at 37 °C for 30 min. After washes, we amplified the ligated circles with 0.125 U/μl phi29 DNA polymerase (Fermentas) in 50 mM Tris-HCl (pH 7.5), 10 mM $MgCl_2$, 10 mM $(NH_4)_2SO_4$, 250 μM dNTPs, 250 ng/μl BSA and 0.05% Tween-20 at 37 °C for 60 min. We detected the single-stranded RCA products by hybridization with 6.25 nM fluorescence-labeled probe Alexa 555-CAGTGAATGCGAGTCCGTCT (MWG-BIOTECH) in 2× SSC, 7.5 ng/μl poly(A), 250 ng/μl BSA and 0.05% Tween-20 for 30 min at 37 °C. For the experiment in **Figure 2e**, we also used the fluorescence-labeled probe Cy5-AGCGATCTGCGAGACCGTAT. We then stained the slides with a mouse antibody to actin (Cederlane Labs), followed by incubation with FITC-labeled rabbit-anti-mouse antibody (Jackson ImmunoResearch) or FITC-labeled antibody to CD45 (Dako) and subsequent counterstaining with 1 μM Hoechst 33342 (Sigma).

Conventional immunostaining (used in **Fig. 3b**) was performed by staining with antibody to c-Myc and EnVision+ System-HRP (DAB; Dako) according to the staining protocol provided by the manufacturer, followed by counterstaining with Mayer hematoxylin (see also **Supplementary Protocol**).

**Image analysis.** We used an epifluorescence microscope (Axioplan II, Zeiss), equipped with a 100-W mercury lamp, a charge-coupled device camera (C4742-95, Hamamatsu) and a computer-controlled filter wheel with excitation and emission filters for visualization of DAPI, FITC, Cy3 and Cy5. We used a ×63 objective (Plan-Neofluar, Zeiss) for all images, except in **Figure 3** (×40, Plan-Neofluar). We collected images using the Imstar software (Imstar), and the AxioVision LE 4.3 software (Zeiss) and thresholded them using Adobe Photoshop CS (Adobe Systems). To further increase the contrast of the images, we multiplied the readings in the green and blue channels by the inverse value of the red channel using a MATLAB 7.0 script (MathWorks). Similarly, we multiplied the values in the green channel by the inverse value of the blue channel. For quantitative measurements, we stored data in a 24-bit RGB TIF file and analyzed them using dedicated software written in MATLAB 7.0. Briefly, the software applied a user-defined threshold on the specific nuclear or cytoplasmic colored layers to identify each cell

or compartment and subsequently identified and counted single-molecule objects within each compartment by applying a second user-defined threshold. We removed isolated single pixels from the binary mask to filter out detector noise.

**Statistical analysis.** We used the GraphPad 4.0 software (GraphPad). Statistical significance was accepted when $P < 0.05$ using one-tailed Student *t* test when comparing two groups and analysis of variance with Dunnett's correction when comparing more than two groups. Values are presented as means ± s.d.

*Note: Supplementary information is available on the Nature Methods website.*

**ACKNOWLEDGMENTS**

We thank A.-C. Andersson for technical assistance; C. Wählby for image analysis; M. Taussig and S. Fredriksson for valuable comments on the manuscript; J.M. Sedivy and M. Eilers for providing cells; A.-C. Steffen and J. Carlsson for providing EGFR and Her-2 antibodies; and G.R. Adolf for providing IFN-γ. We obtained frozen human tissues from the Fresh Tissue Biobank at the Department of Clinical Pathology, Uppsala University Hospital (supported by the SWEGENE/Wallenberg Consortium North Biobank Program). This project was supported by the Wallenberg Foundation, the EU Integrated Project MolTools, the Research Councils of Sweden for natural science and for medicine (to U.L.); and the Swedish Cancer Foundation, the Swedish Children Cancer Foundation and the Human Frontiers Science Program (to L.-G.L.).

**COMPETING INTERESTS STATEMENT**

The authors declare competing financial interests (see the *Nature Methods* website for details).

**Published online at http://www.nature.com/naturemethods/**
**Reprints and permissions information is available online at http://npg.nature.com/reprintsandpermissions/**

1. Fredriksson, S. *et al.* Protein detection using proximity-dependent DNA ligation assays. *Nat. Biotechnol.* **20**, 473–477 (2002).
2. Gullberg, M. *et al.* Cytokine detection by antibody-based proximity ligation. *Proc. Natl. Acad. Sci. USA* **101**, 8420–8424 (2004).
3. Baner, J., Nilsson, M., Mendel-Hartvig, M. & Landegren, U. Signal amplification of padlock probes by rolling circle replication. *Nucleic Acids Res.* **26**, 5073–5078 (1998).
4. Grandori, C., Cowley, S.M., James, L.P. & Eisenman, R.N. The Myc/Max/Mad network and the transcriptional control of cell behavior. *Annu. Rev. Cell Dev. Biol.* **16**, 653–699 (2000).
5. Oster, S.K., Ho, C.S., Soucie, E.L. & Penn, L.Z. The myc oncogene: MarvelouslY Complex. *Adv. Cancer Res.* **84**, 81–154 (2002).
6. Patel, J.H., Loboda, A.P., Showe, M.K., Showe, L.C. & McMahon, S.B. Analysis of genomic targets reveals complex functions of MYC. *Nat. Rev. Cancer* **4**, 562–568 (2004).
7. Pelengaris, S., Khan, M. & Evan, G. c-MYC: more than just a matter of life and death. *Nat. Rev. Cancer* **2**, 764–776 (2002).
8. Hu, C.D., Chinenov, Y. & Kerppola, T.K. Visualization of interactions among bZIP and Rel family proteins in living cells using bimolecular fluorescence complementation. *Mol. Cell* **9**, 789–798 (2002).
9. Venetsanakos, E. *et al.* Induction of tubulogenesis in telomerase-immortalized human microvascular endothelial cells by glioblastoma cells. *Exp. Cell Res.* **273**, 21–33 (2002).
10. Grinberg, A.V., Hu, C.D. & Kerppola, T.K. Visualization of Myc/Max/Mad family dimers and the competition for dimerization in living cells. *Mol. Cell. Biol.* **24**, 4294–4308 (2004).
11. Winqvist, R., Saksela, K. & Alitalo, K. The myc proteins are not associated with chromatin in mitotic cells. *EMBO J.* **3**, 2947–2950 (1984).
12. Mateyak, M.K., Obaya, A.J., Adachi, S. & Sedivy, J.M. Phenotypes of c-Myc-deficient rat fibroblasts isolated by targeted homologous recombination. *Cell Growth Differ.* **8**, 1039–1048 (1997).
13. Alroy, I. & Yarden, Y. The ErbB signaling network in embryogenesis and oncogenesis: signal diversification through combinatorial ligand-receptor interactions. *FEBS Lett.* **410**, 83–86 (1997).
14. Bouchard, C., Marquardt, J., Bras, A., Medema, R.H. & Eilers, M. Myc-induced proliferation and transformation require Akt-mediated phosphorylation of FoxO proteins. *EMBO J.* **23**, 2830–2840 (2004).
15. Adhikary, S. & Eilers, M. Transcriptional regulation and transformation by Myc proteins. *Nat. Rev. Mol. Cell Biol.* **6**, 635–645 (2005).
16. Öberg, F., Larsson, L.G., Anton, R. & Nilsson, K. Interferon gamma abrogates the differentiation block in v-myc-expressing U-937 monoblasts. *Proc. Natl. Acad. Sci. USA* **88**, 5567–5571 (1991).
17. Guzhova, I. *et al.* Interferon-gamma cooperates with retinoic acid and phorbol ester to induce differentiation and growth inhibition of human neuroblastoma cells. *Int. J. Cancer* **94**, 97–108 (2001).
18. Bahram, F., Wu, S., Öberg, F., Lüscher, B. & Larsson, L.G. Posttranslational regulation of Myc function in response to phorbol ester/interferon-gamma-induced differentiation of v-Myc-transformed U-937 monoblasts. *Blood* **93**, 3900–3912 (1999).
19. Eilers, M., Picard, D., Yamamoto, K.R. & Bishop, J.M. Chimaeras of myc oncoprotein and steroid receptors cause hormone-dependent transformation of cells. *Nature* **340**, 66–68 (1989).
20. Littlewood, T.D., Hancock, D.C., Danielian, P.S., Parker, M.G. & Evan, G.I. A modified oestrogen receptor ligand-binding domain as an improved switch for the regulation of heterologous proteins. *Nucleic Acids Res.* **23**, 1686–1690 (1995).
21. Solomon, D.L., Philipp, A., Land, H. & Eilers, M. Expression of cyclin D1 mRNA is not upregulated by Myc in rat fibroblasts. *Oncogene* **11**, 1893–1897 (1995).
22. Yin, X., Giap, C., Lazo, J.S. & Prochownik, E.V. Low molecular weight inhibitors of Myc-Max interaction and function. *Oncogene* **22**, 6151–6159 (2003).
23. Arabi, A. *et al.* c-Myc associates with ribosomal DNA in the nucleolus and activates RNA polymerase I transcription. *Nat. Cell Biol.* **7**, 303–310 (2005).
24. Beckstead, J.H. A simple technique for preservation of fixation-sensitive antigens in paraffin-embedded tissues. *J. Histochem. Cytochem.* **42**, 1127–1134 (1994).